

RTD FILE COPY

DEJ

(2)

N66001-80-C-0318 .

AD-A215 443

THE DEVELOPMENT AND DELIVERY OF A LEAD VAPOR
CELL SUITABLE FOR STIMULATED RAMAN SCATTERING

B. G. Bricks
General Electric Company
Space Systems Division
P. O. Box 8555
Philadelphia, PA 19101

September 1981

Final Report for Period September 1980 - September 1981

Prepared for

DEFENSE ADVANCED RESEARCH PROJECTS AGENCY
Directed Energy Office
1400 Wilson Boulevard
Arlington, VA 22209

NAVAL OCEAN SYSTEMS CENTER
271 Catalina Boulevard
San Diego, CA 92152

DTIC
S ELECTE D
NOV 15 1989
Q E

APPROVED FOR PUBLICATION
BY THE DIRECTOR OF THE
DEFENSE ADVANCED RESEARCH PROJECTS AGENCY

89 11 14 002
— — 1

REPORT DOCUMENTATION PAGE		READ INSTRUCTIONS BEFORE COMPLETING FORM
1. REPORT NUMBER	2. GOVT ACCESSION NO.	3. RECIPIENT'S CATALOG NUMBER
4. TITLE (and Subtitle) THE DEVELOPMENT AND DELIVERY OF A LEAD VAPOR CELL SUITABLE FOR STIMULATED RAMAN SCATTERING		5. TYPE OF REPORT & PERIOD COVERED FINAL REPORT 9/80-9/81
		6. PERFORMING ORG. REPORT NUMBER
7. AUTHOR(s) B. G. Bricks		8. CONTRACT OR GRANT NUMBER(s) N66001-80-C-0318
9. PERFORMING ORGANIZATION NAME AND ADDRESS General Electric Company Space Systems Division P.O.Box 8555, Philadelphia, PA 19101		10. PROGRAM ELEMENT, PROJECT, TASK AREA & WORK UNIT NUMBERS
11. CONTROLLING OFFICE NAME AND ADDRESS DARPA Directed Energy Office 1400 Wilson Blvd., Arlington, VA 22209		12. REPORT DATE SEPTEMBER 1981
		13. NUMBER OF PAGES
14. MONITORING AGENCY NAME & ADDRESS (if different from Controlling Office) Naval Ocean Systems Center 271 Catalina Blvd. San Diego, CA 92152		15. SECURITY CLASS. (of this report) UNCLASSIFIED
		15a. DECLASSIFICATION/DOWNGRADING SCHEDULE
16. DISTRIBUTION STATEMENT (of this Report)		
17. DISTRIBUTION STATEMENT (of the abstract entered in Block 20, if different from Report)		
18. SUPPLEMENTARY NOTES		
19. KEY WORDS (Continue on reverse side if necessary and identify by block number) Lead Vapor, Stimulated Raman Scattering; Heat Pipe, Wicks; High Temperature.		
20. ABSTRACT (Continue on reverse side if necessary and identify by block number) A high temperature, lead vapor cell for use in stimulated Raman scattering of XeCl laser radiation was designed, manufactured, tested and delivered. Recirculating wick structures were used for metal vapor confinement. During a performance life test, 835 hours of continuous operation was achieved with a lead vapor density $\geq 1.6 \times 10^{17}/\text{cm}^3$ (1270°C equivalent temperature) in an active volume 2.5 cm by ~85 cm.		

SUMMARY

This report describes the results of a program to design, manufacture, test and deliver a lead vapor cell suitable for use in the frequency down-conversion of XeCl laser light by means of stimulated Raman scattering. The principal objective of the program was to demonstrate that the heat pipe techniques used for the confinement of high temperature lead vapor in a lead vapor laser can be adapted to this application and produce long life operation. The specific goals were to achieve a temperature of 1200°C (lead density = $2 \times 10^{17}/\text{cm}^3$) over a length $\ell_0 \geq 60$ cm ($\text{pd} = 1.2 \times 10^{19}/\text{cm}^2$) for a minimum operating time of 500 hours.

The cell was designed using a high density ceramic tube with demountable window assemblies and a commercial high temperature process tube furnace. An optical absorption system was designed and implemented in order to monitor the lead vapor density in the cell. Two types of wicking materials for capture and recirculation of the metal were tested. One material (W) was determined unacceptable, but the second (WC) produced exceptional test results.

A long life test was run for a continuous period of 835 hours during which the lead vapor density varied from 1.7 - $1.6 \times 10^{17}/\text{cm}^3$. This corresponds to an equivalent operating temperature of $\sim 1270^{\circ}\text{C}$. Since the hot zone was ~ 85 cm long the pd product varied from 1.45 - $1.6 \times 10^{19}/\text{cm}^2$. It was necessary to terminate the test at that elapsed time in order to hold the contract within cost and schedule. A least squares fit to the data of lead density as a function of time during the 835-hour run predicts a useful operating life of 3900 hours if one selects a $\text{pd} = 1.2 \times 10^{19}/\text{cm}^2$ as the cutoff point. If the cutoff is lowered to $1.0 \times 10^{19}/\text{cm}^2$, a factor of 20% below the contract goal, the predicted operating life is 7500 hours.

TABLE OF CONTENTS

SUMMARY	ii
1.0 INTRODUCTION	1
2.0 TECHNICAL BACKGROUND: VAPOR CONFINEMENT IN METAL VAPOR LASERS.	2
3.0 SYSTEM DESIGN.	6
3.1 Furnace Description.	6
3.2 Cell Design.	7
4.0 TEST PROGRAM	12
4.1 Furnace Installation	12
4.2 Thermal Profile Along Wicks.	13
4.3 Measurement of Lead Vapor Density by Optical Absorption.	16
4.4 Cell Preparation	24
4.5 Lead Vapor Cell Test Program	25
5.0 CONCLUSIONS AND RECOMMENDATIONS.	30
ACKNOWLEDGMENTS.	31
REFERENCES	32
APPENDIX: INSTALLATION/OPERATION INSTRUCTIONS.	33

Accession For	
NTIS GRA&I	<input checked="" type="checkbox"/>
DTIC TAB	<input type="checkbox"/>
Unannounced	<input type="checkbox"/>
Justification	
By	
Distribution/	
Availability Codes	
Dist	Avail and/or Special
A-1	

LIST OF ILLUSTRATIONS

Figure 1.	The lead vapor cell, high temperature furnace and vacuum/gas handling system.	8
Figure 2.	Details of the window assemblies.	10
Figure 3.	Temperature profile along the cell tube as it passes through the end walls of the furnace	15
Figure 4.	Energy level diagram of the lead atom	17
Figure 5.	Vapor pressure of lead and the corresponding number density as a function of temperature . . .	18
Figure 6.	Population of the $6p^2\ ^3P_2$ state of the lead atom as a function of temperature	19
Figure 7.	Optical system used for the measurement of lead density by optical absorption.	21
Figure 8.	The percent absorption at line center of the 405.7 nm line as a function of lead atom number density	23
Figure 9.	The percent absorption as a function of time during the 835-hour life test.	28

LIST OF TABLES

Table 1.	Design Criteria for the Lead Vapor Raman Cell . .	6
Table 2.	Percent Absorption at 405.7 nm Line Center. . . .	22

1.0 INTRODUCTION

Certain proposed Navy programs require laser sources emitting in the blue-green region of the spectrum. This need has motivated development programs over the last several years to evaluate the feasibility of candidate laser systems.⁽¹⁾ One of the promising laser systems to emerge from this effort is the rare-gas halide XeCl₂. This laser satisfies several of the basic performance requirements, but its laser line is at 308 nm in the uv and far removed from the blue-green. Therefore, it must be frequency shifted to the proper region with a high conversion efficiency if XeCl₂ is to be a viable blue-green laser system.

Efficient frequency down-conversion has been demonstrated in several atomic⁽²⁾ and molecular gases by means of stimulated Raman scattering. Conversion efficiencies of 40-50% of the XeCl₂ emission have been achieved using this technique in lead vapor at concentrations on the order of 10^{16} - 10^{17} cm⁻³ (1200-1300°C).

Thus in order to have a blue-green laser system which meets the practical performance criteria, the problem of frequency down-conversion becomes one of maintaining a high lead vapor pressure (~30 torr, 1300°C) for extended periods of time (multi-hundred to thousands of hours). It is the goal of this program to apply the techniques used for vapor confinement in lead vapor lasers^(3,4) under less stressful conditions (0.5-1.0 torr, 925-950°C), to evaluate them for this system operating regime and finally to demonstrate long term operation (500 hours). Success in meeting or exceeding these goals would have a significant impact on the blue-green laser programs.

(1) R.Burnham and E.Schimitschek, "High Power Blue-Green Lasers," Laser Focus 17, 54 (1981).

(2) R.Burnham and N.Djeu, "Efficient Raman Conversion of XeCl₂-Laser Radiation in Metal Vapors," Optics Letters 3, 215 (1978).

(3) B.G.Bricks, "Development of the Discharge-Heated Lead Vapor Laser," AFAL-TR-78-103, Air Force Avionics Laboratory, Wright-Patterson AFB, OH 45433, 1978.

(4) T.W.Karras and B.G.Bricks, "Metal Vapor Laser Contaminant Study," GE TIS No. 80SDS028, October 1980.

2.0 TECHNICAL BACKGROUND: VAPOR CONFINEMENT IN METAL VAPOR LASERS

The frequency down-conversion of the XeCl laser emission at 308 nm in the uv to 459 nm in the blue-green region of the spectrum has been efficiently accomplished by stimulated Raman scattering in a lead vapor cell. Scattering is first observed in a cell containing a buffer gas and a partial pressure of lead of about 1 torr or greater. In order to achieve this lead vapor concentration the active zone of the cell must be kept in the temperature range of 1000-1100°C. Since conversion efficiency improves with increased lead vapor concentrations, it is desirable to operate a cell at about 30 torr or 1300°C. Under these operating conditions the useful operating life of a Raman cell is limited by the strong thermal and concentration gradient diffusion forces which deplete the active hot zone of metal vapor.

Similarly, one of the principal requirements for a practical metal vapor laser system is the long term confinement of the metal vapor within the active hot zone of the laser discharge tube. A typical discharge tube for the GE-SSD metal vapor lasers is made from high density ceramic (Coors AD998) and is approximately 100 cm long with an inner diameter in the range of 2.5 to 4.0 cm. Since the central zone of the discharge tube must be at elevated temperatures for laser operation (950°C for lead and 1400°C for copper) and the end window assemblies are close to room temperature, there is necessarily a large thermal and concentration gradient at each end of the discharge tube. This gradient eventually degrades laser performance due to metal loss and local condensation buildup of the metal in the cooler region which apertures the beam.

At GE-SSD techniques from heat pipe technology have been selectively adapted to the metal vapor laser to minimize these deleterious effects by containing the metal vapors within the hot active zone of the laser tube. The similarity in geometry, working material, and temperature profile between a metal vapor laser discharge tube and a Raman scattering cell suggests that the

metal confinement techniques of the lasers may be applied equally well to the lead vapor Raman cell.

In the metal vapor laser discharge tube a recirculating wick structure is placed in each end. The normal thermal gradient at the ends is specially tailored to produce a proper temperature distribution along the length of the wick so that it will collect, condense and return the liquid metal to the hot zone by capillary forces.

The approach is obviously quite analogous to that of a heat pipe, but certainly not identical to it. For example:

- 1) the cylindrical wicks are placed in both ends of a discharge tube, but they must not occupy a significant fraction of the length of a tube otherwise the pulsed electrical discharge for laser excitation will be shorted out.
- 2) since the ends must be open for operation of a laser there will be a very small, but finite, loss of working medium out of the ends of the wicks.
- 3) little heat transfer is accomplished (or desired) because of the high buffer gas pressures required for discharge operation and the relatively low density (temperature) of the working medium.

For the laser applications rigid porous structures have been selected to provide the wicking action. The strength or rigidity is an important criteria because the combination of high temperatures, the high surface tension forces of the liquid metals and exposure to the high intensity pulsed electrical discharge will gradually distort more flexible wire or thin foil wicks. This not only eventually results in wick failure, but in the laser application any distortion which pulls the wick away from the inner wall of the discharge tube will aperture the beam and degrade laser output power and beam quality.

In the other important characteristics, such as having small passages to enhance the capillary action, proper wetting and

materials compatibility, the laser wick requirements clearly are the same as for heat pipe.

In the case of heat pipes the wicking structure extends the entire length of the device with evaporation at one end, condensation at the opposite end and an adiabatic zone separating them. In the laser application the wicks occupy only a small percentage of the length of the tube. The purpose of the high temperature or evaporative end is to maintain the proper working partial pressure in the laser active zone in the central region of the tube. This is, in general, at most one to two inches of wick length. The function of the remainder of the wick is to capture and recirculate the metal vapor as it diffuses through the wick to the cooler regions of the tube.

To our knowledge no theoretical investigation of this diffusion process and the capture ability of the wick and its fluid metal transport properties under these conditions has been undertaken in order to predict the confinement times. Furthermore, it was beyond the scope of this program to do so. However, the data accumulated in numerous experiments in our laboratory and others have provided an empirical relationship between confinement time (defined as laser operating time) and the length-to-diameter ratio of the wicks. This relationship has been used to select the wick length for the current application.

The first confinement experiments in a lead laser used sintered nickel wicks. This material exhibited excellent wetting characteristics with lead, but wick failure occurred in 100 hours or less. This was attributed to the relatively high solubility of lead and nickel at the laser operating temperature of 950°C .

More recent work with wicks for lead has concentrated on refractory metals because of their superior characteristics at high temperature and no solubility with lead. For example, wicks have been manufactured by plasma spraying a 0.005 to 0.010 inch layer of tungsten on tantalum sheet.

This method greatly reduces the manufacturing cost and also increases the flexibility for design changes. Since the sheets can be sprayed in pieces of reasonable size, they can be cut and rolled to form tubes of different diameter. Similarly it is easy to fashion wicks of various lengths.

This type of wick has operated successfully in a lead laser for periods of approximately 100 hours in both a sealed and non-sealed mode. Based on these positive results this wick type was selected for the first tests on the current program.

3.0 SYSTEM DESIGN

The objective of this program was to design a lead vapor cell for Raman frequency down-conversion, purchase all necessary components and materials, manufacture, test and deliver the cell. The basic design criteria for the cell are listed in Table 1.

TABLE 1. DESIGN CRITERIA FOR THE
LEAD VAPOR RAMAN CELL

Cell Diameter:	2.5 cm
Cell Length - Active Hot Zone:	60 cm
- Overall Length:	~6 ft
Operating Temperature:	1300°C
Operating Life:	500 hr

As the discussion in the previous two sections has indicated, it was also intended that the design of the cell rely heavily upon the techniques which have been used successfully at GE-SSD in the metal vapor lasers. In the remainder of this section we shall elaborate the design of the cell in some detail.

3.1 FURNACE DEFINITION

In the GE-SSD metal vapor lasers the proper operating temperature (metal vapor density) for the tube is obtained by using the waste heat from the pulsed electrical discharge. Since the Raman cell is a passive device with no discharge present a furnace is required to heat the cell to the desired working temperature. The first three characteristics listed in Table 1 determine the base line for definition of the furnace. A commercially-available process tube furnace and controller were selected for this program. They are a Lindberg process furnace model 54279 and a control console model 59545-A.

The furnace will accept a 2 inch OD working tube. This dimension allows some flexibility for mounting and supporting the 1-1/4 inch OD Raman cell tube. It also may permit the use of slightly larger diameter tubes for the cell if such a change is desired in the future.

The furnace has a total hot zone length between the end walls of 36 inches. Power is applied to the heater elements which are grouped in three independently controlled zone heater units. This overall hot zone length is 50% greater than the value called out in Table 1, but it was decided that this margin was required to ensure that a length greater than 24 inches could be maintained at the desired operating temperature if there was a significant roll-off near the end walls of the furnace.

The heater elements for the furnace are silicon carbide rods which give it a maximum operating temperature of 1500°C . This capability also provides margin so that 1300°C can be achieved easily for extended periods of time.

3.2 CELL DESIGN

The design of the high temperature, lead vapor cell is based heavily on the metal vapor laser discharge tubes. A schematic of the cross-section of the cell and the process furnace is shown in Figure 1. The sketch of the cell is to scale along the main axis of the furnace but not in the transverse direction.

The main tube of the cell is made from high density alumina (Coors AD998) with dimensions 1 inch ID, 1-1/4 inch OD, and 72 inches long. The overall furnace length is 46 inches, allowing 13 inches of the tube to extend out each end. The tube is located on the axis of the furnace by alumina support rings at the outer ends of the firebrick end walls. As can be seen in the figure, a second alumina tube of larger diameter is also supported by alumina rings in the end walls and on the support columns which are an integral part of the furnace.

The outer tube serves as a protective jacket for the main cell tube. During the first two tests of the cell (without this second outer tube) the main tube developed a series of incipient cracks on its underside. These tubes eventually developed vacuum leaks and fractured when a slight mechanical stress was applied. This phenomena has never been observed with these tubes in a laser environment despite the existence of similar or worse thermo/mechanical stresses. We implemented the protective jacket tube

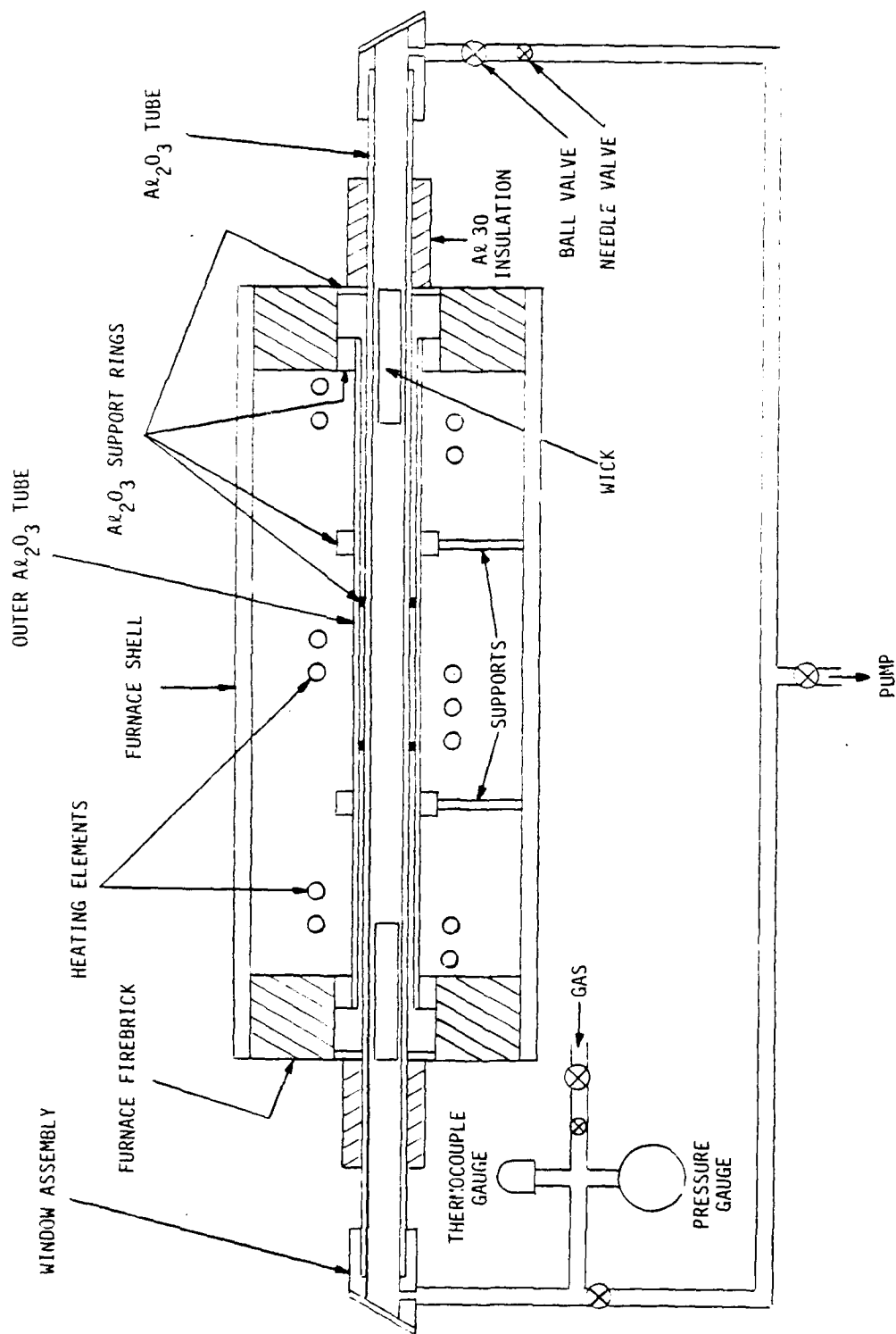


Figure 1. The lead vapor cell, high temperature furnace and vacuum/gas handling system are shown schematically. The cross section of the cell and the furnace is to scale lengthwise but not in the vertical.

to keep the main cell tube from looking directly at the heater rods and the interior of the furnace. Even though the failure mechanism(s) have not been defined, since this corrective action was taken no additional failures have occurred.

Window assemblies are required for direct mounting on the ends of the cell tube and must provide the following functions: 1) vacuum tight connection to the alumina tube, 2) vacuum/gas line connections, and 3) support for high quality optical windows, preferably demountable for ease in cleaning and/or replacement if required.

The window assembly design is shown in Figure 2. The pair of assemblies was manufactured in our in-house model shop. The seal to the alumina tube is by the tapered "O"-ring compression fitting. The tapered compression ring is necessary to accommodate the rather large variation in dimensions of the tubes as they are received from the vendor. Since the ID of the window assembly also had to be oversized to accommodate the variation in tube dimension a second "O"-ring, which performs no sealing function, was included to keep the assembly in coaxial alignment with the tube. The optical windows (Esco, quartz, 1/4 wave) are sealed with a standard "O"-ring design. Vacuum/gas line connections are made through the 1/8 inch pipe thread in each assembly.

The vacuum/gas handling system is also shown schematically in Figure 1. A Welch model 1397 fore pump is used to evacuate the cell and lines. Ultimate pump down pressures are measured by a Hastings DV-5M, 0-100 micron thermocouple gauge. After out-gassing of the ceramic tube at 1300°C and the external tubing with hot air guns, ultimate pressures in the range of 2-4 microns were achieved. The cell showed no leak on the 10^{-9} std cc/sec scale of a helium leakchecker.

Appropriate valving was included to be able to isolate the cell from the vacuum pump. A manifold was assembled to permit the use of different buffer gases and mixtures. The pressure of the buffer gas is measured by a Wallace and Tiernan model 61-1D-0200, 0-200 mm pressure gauge.

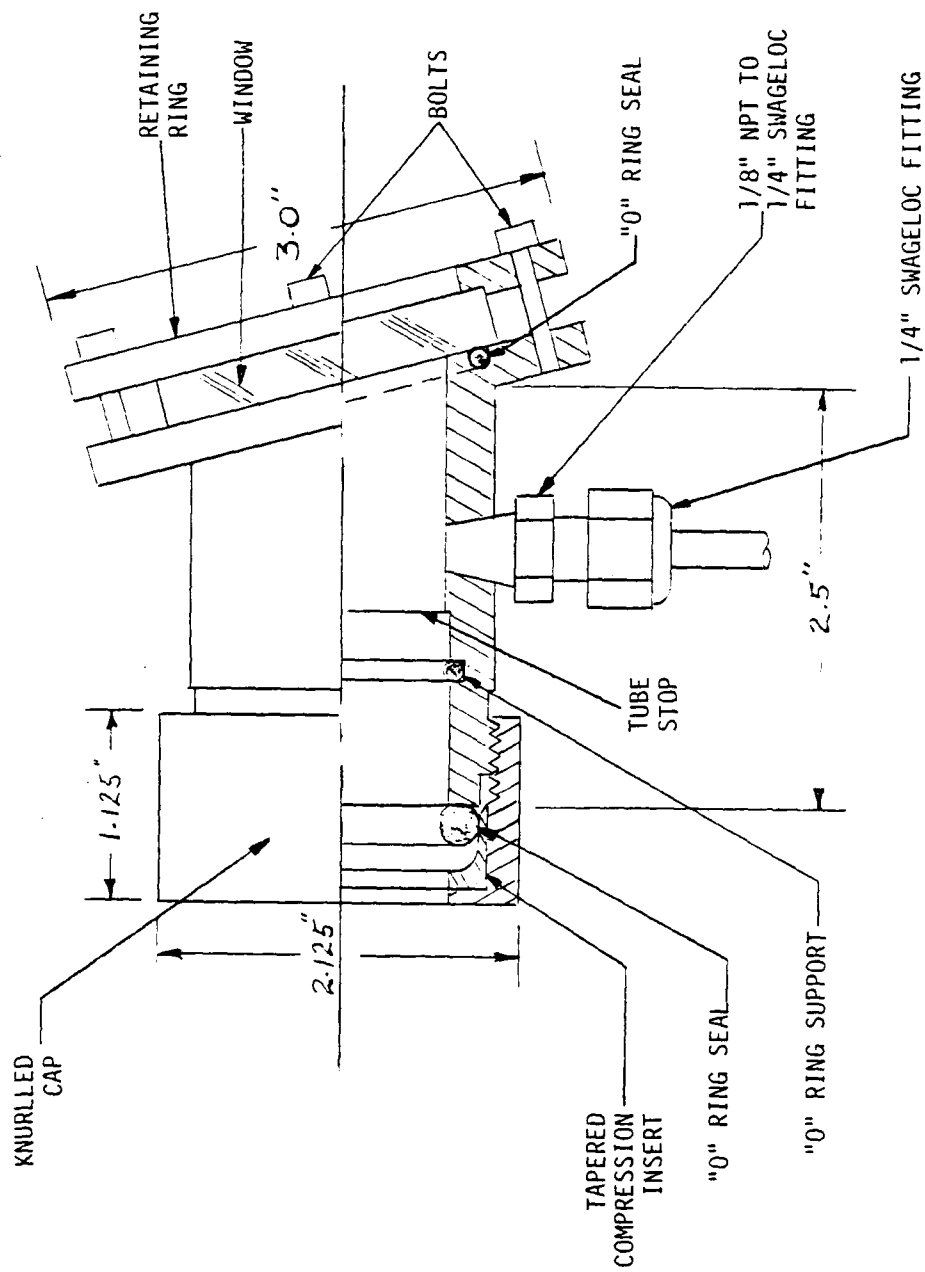


Figure 2. Details of the window assemblies (to scale).

The important remaining design characteristic of the cell is the length and material composition for the recirculating wick. The length of the wicks was chosen to be 8 inches. This is based on two criteria. The first is the empirical relationship which has been generated by work in this laboratory between the length-to-diameter ratio (L/D) of the wick and the operating life of the metal vapor laser. If this relationship can be directly applied to the conditions encountered for the Raman cell, then an 8-inch long wick ($L/D=8$) should result in a multi-hundred hour lifetime.

The second determining factor is the temperature roll-off profile at the ends of the furnace since the gradient affects performance, and the point at which the temperature goes below the freezing point of lead will determine the maximum length. The 8-inch length is also consistent with roll-off profile at the end of the furnace. (The details of the measurement of this profile are discussed in Section 4.2.)

The choice of materials for the wicks was based on prior experience in the metal vapor lasers. Since plasma-sprayed tungsten on a tantalum substrate has performed in the laser environment it was chosen as the first composition to be tested.

A sintered tungsten wick would have been investigated, but the vendor could not fabricate them 8 inches long. This, coupled with their high cost, ruled out their use at this time. However, it is believed that this type has certain definite merits and should indeed be included for testing in the future.

Work on some early metal vapor laser programs in this laboratory showed that the carbides of some refractory metals have superior wetting characteristics to the pure metals themselves. Therefore, the second composition chosen to be tested in this program was plasma-sprayed tungsten carbide on a tantalum substrate.

A third type could not be tested because the test program had to be reduced in scope. This action was required due to a large unexpected cost growth incurred during installation of the furnace.

4.0 TEST PROGRAM

4.1 FURNACE INSTALLATION

The high temperature furnace was installed in one of the laser test laboratories on a 4'x8' air-suspension optical table. This type of table provided a suitably sturdy mounting platform for the furnace which weighs several hundred pounds as well as space for setting up some of the optical diagnostic equipment described in Section 4.3.

The following tasks were required to bring the furnace on-line:

- 1) wire control console to house power;
- 2) wire control console to furnace;
- 3) placing, packing and wiring the 32 silicon carbide heater elements in their individual mounting holes.

After completion of the above tasks, each attempt to follow the initial heat-up cycle called out by the manufacturer was terminated by the breakage of one or more heater rods. This problem persisted and was eventually traced, through a combined diagnostic effort of both GE and vendor personnel, to a manufacturing defect in the furnace.

Each heater element is mounted transverse to the main axis of the furnace and is supported at each of its ends in holes which pass completely through the firebrick sidewalls of the furnace. The rods are a nominal 1/2 inch in diameter, and the mounting holes are a nominal 3/4 inch diameter. Each rod is located on the axis of its mounting holes by loosely packing the annular clearance region with fibrous alumina.

It was discovered that the pairs of mounting holes for each and every heater rod were misaligned by approximately 1° . This misalignment, coupled with the close fit of the elements in the holes and the growth of all furnace components on heating, was sufficient to put transverse stresses on some of the rods and fracture them. The problem was most severe towards the ends of the furnace.

The problem was corrected by simultaneously boring out each pair of holes to an oversize diameter with a large piece of drill rod. This increased the clearance and also essentially brought the holes into angular alignment. Following this corrective action satisfactory furnace operation was achieved. No further breakage has occurred despite numerous thermal cycles, including many to room temperature, which is particularly stressful to the heater rods. This problem did, however, have a serious impact on both the program schedule and cost.

4.2 THERMAL PROFILE ALONG WICKS

The operation of the wick material as a container of high temperature metal vapor requires a proper temperature distribution along the length of the wick. The inboard end of the wick must be in the operating zone at the desired temperature and capable of a net vaporization rate into the active zone to balance the loss of vapor by diffusion to the cooler zones of the wick. The remainder of the wick must efficiently capture and condense out this vapor diffusing through it, and wick the liquid metal back to the hot zone at a rate equal to the vaporization rate. The outboard end of the wick must be above the melting point of the metal in question, but not sufficiently high to vaporize significant quantities of metal into the zone beyond the wick where it is lost. If this occurs the wick obviously ceases to function efficiently in its primary role as a metal vapor container. Since, in general, wetting forces are greater at high temperature, the thermal gradient across the length of the wick causes the liquid metal to be wicked from the cooler to the hotter regions of the wick.

In the discharge-heated metal vapor lasers the proper temperature profile along the wicks is empirically determined by adjusting both the position of the wick in the discharge tube and the heat shielding exterior to the tube. The use of a furnace reduces this flexibility because the principal thermal gradient occurs through the firebrick end wall of the furnace, and there are no simple changes which can be made to alter it significantly.

Since the wicks are placed deep inside the cell (Figure 1) repositioning is very difficult. Also the scope and size of the program placed severe limitations on the number of tests which could be performed. Therefore, it was decided to measure the temperature profile along a cell tube as it exits the furnace;* and locate the wicks accordingly.

Following the initial bakeout of the furnace (with no process tube in place, as per instructions), a cell tube was instrumented with five thermocouples positioned as shown in Figure 3. The thermocouples were bonded to the cell tube with Zircar alumina cement. The temperature of the furnace was increased from 800°C to 1300°C in 100°C increments, and the temperature was monitored at each thermocouple. The experiment was performed with and without an insulator sleeve covering the process tube within the opening in the firebrick end wall. A portion of this data is plotted in Figure 3.

From the curves it can be seen that the wall temperature of the cell tube is equal to the furnace temperature setting approximately one inch inside the end wall. With the furnace at 1300°C the tube temperature passes below the melting point of lead approximately one inch outside the firebrick end wall.

Based on this information a wick length of 8 inches was chosen. Thus a wick would extend from one inch outside the end wall to two inches inside the end wall which should ensure the inboard end of the wick being at the furnace temperature. In actual practice we have placed the wicks approximately one inch further in so that the outboard end is coincident with the end of the furnace. The roughly linear roll-off in temperature should ensure good wicking action, and according to the empirical relationship the L/D ratio of eight should produce multi-hundred hour operation.

*In the lasers empirical changes are actually easier to make than with the furnace, but temperature profile measurements are not because electrical leads must be brought out through the vacuum jacket and there is interference from the pulsed electrical discharge.

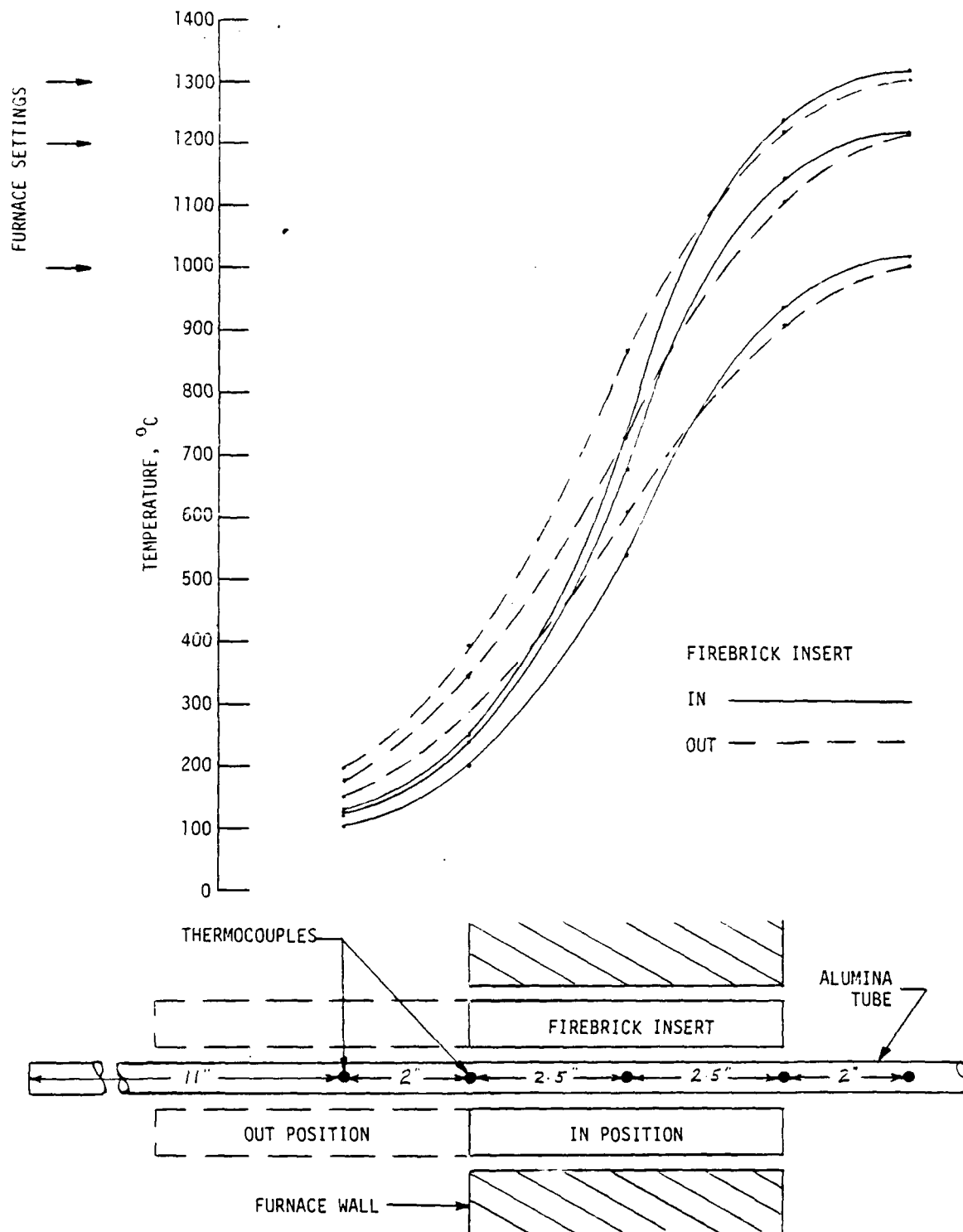


Figure 3. Temperature profile along the cell tube as it passes through the end walls of the furnace.

4.3 MEASUREMENT OF LEAD VAPOR DENSITY BY OPTICAL ABSORPTION

When recirculating wicks are used as metal vapor confinement devices in metal vapor lasers, the existence of laser oscillation, the level of performance and the operating lifetime before reloading or replacement constitute criteria or figures of merit for the wicks. However, in the current system in our laboratory no such operating parameters exist to monitor the performance of the wicks. Therefore an independent method is required to measure the lead vapor density as a function of time.

It was decided that the most promising technique to provide such a monitor would be the use of optical absorption on one or more of the lines of lead. An examination of the abbreviated energy level diagram for the lead atom (Figure 4) reveals two low lying energy levels ($6p^2\ ^3P_1$ and $6p^2\ ^3P_2$) approximately 1 eV above the ground state which should have significant thermal population at 1300°C .

The vapor pressure of lead as a function of temperature was taken from reference 5 and is plotted in Figure 5. This data was also converted to number density as a function of temperature using the ideal gas law, and this data is also included in the figure. Using the Boltzmann distribution

$$n_1 g_1 = N_0 g_0 e^{-E_1/kT} \quad (1)$$

the population density for the $6p^2\ ^3P_2$ state was calculated over the range of interest and is plotted in Figure 6. Clearly the densities are large enough that a high degree of absorption would be expected on the 405.7 nm line.

The absorption coefficient at line center, α_0 , was estimated for the 405.7 nm line using the expression

$$\alpha_0 = \sqrt{\frac{\ln 2}{\pi}} \frac{g_2 A_{21}}{8\pi} \frac{n_1}{g_1} \frac{\lambda^2}{\Delta\nu_D} \quad (2)$$

(5) R.E.Honig and D.A.Kramer, "Vapor Pressure Data for the Solid and Liquid Elements," RCA Review, 296 (June 1969).

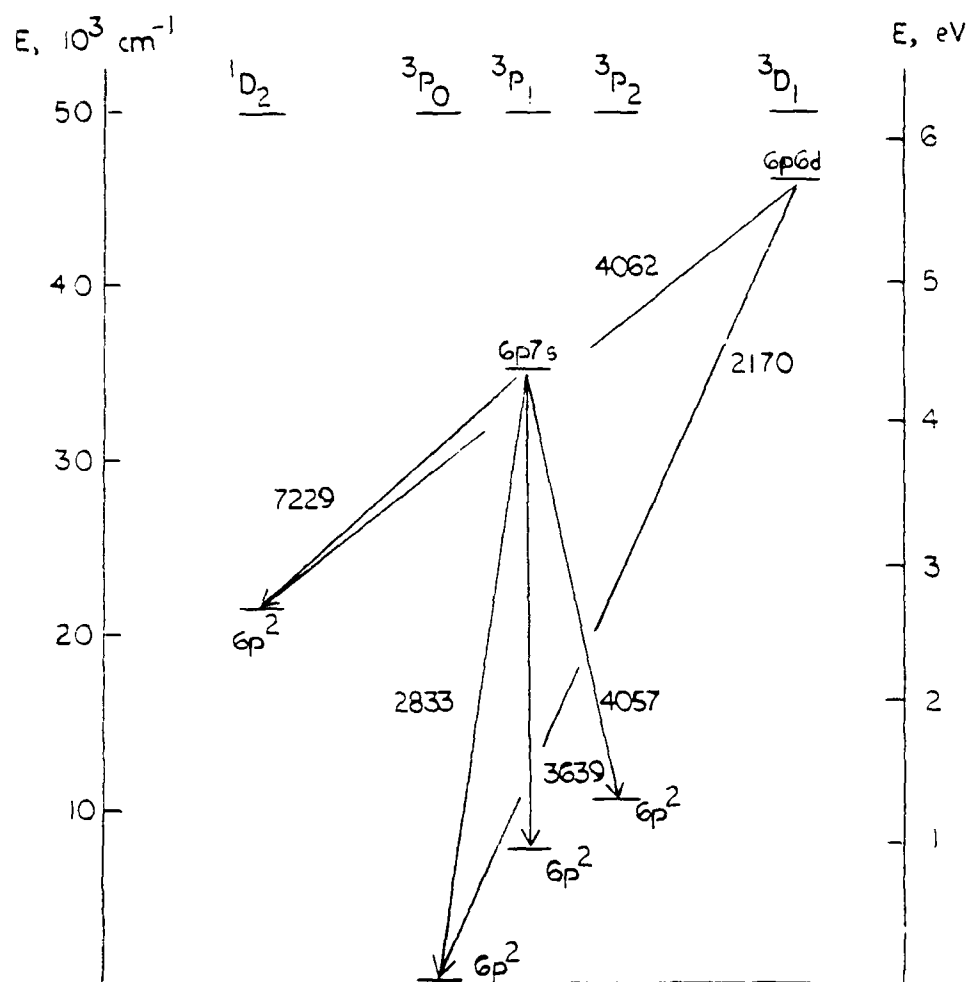


Figure 4. Energy level diagram of the lead atom.

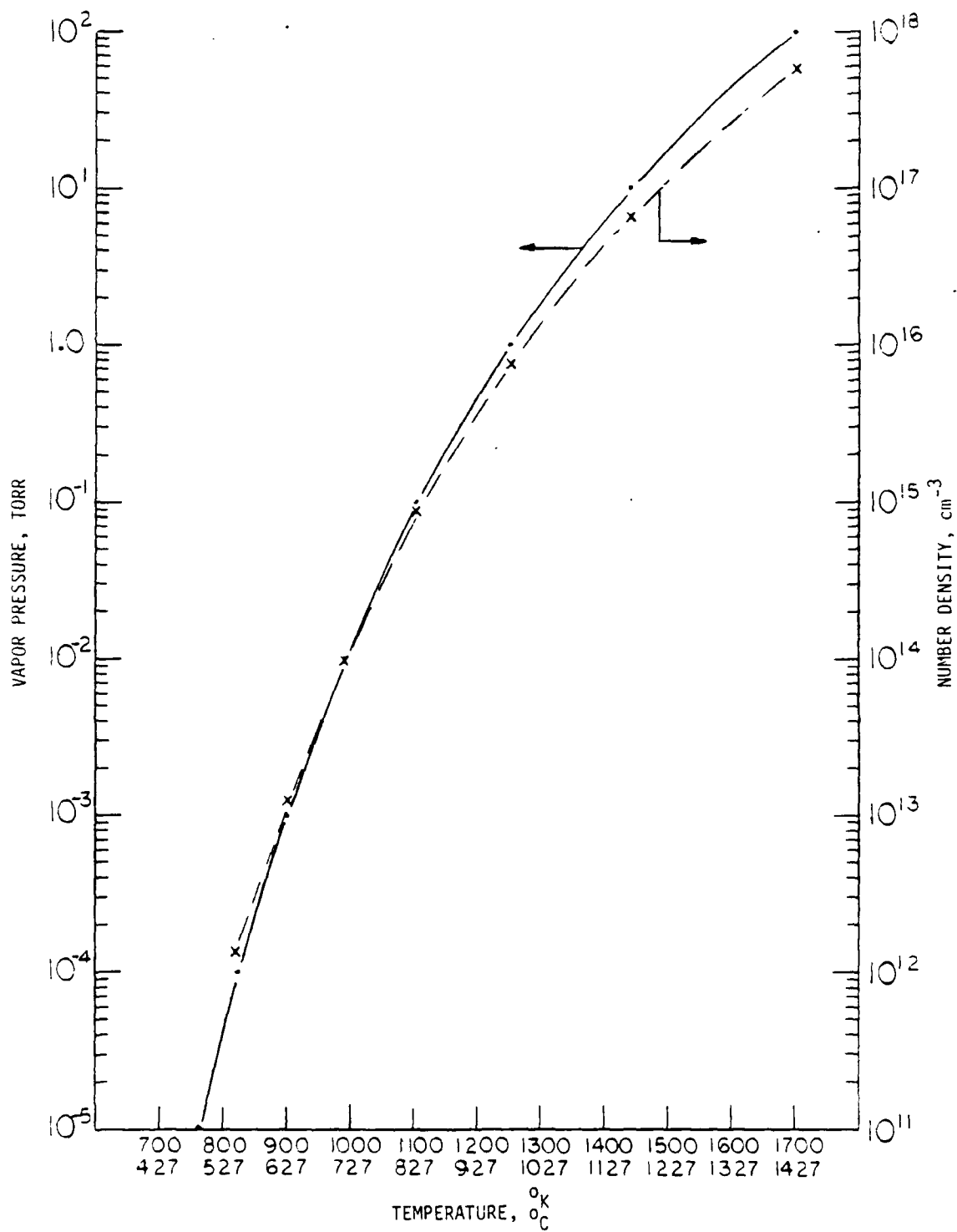


Figure 5. Vapor pressure of lead and the corresponding number density as a function of temperature.

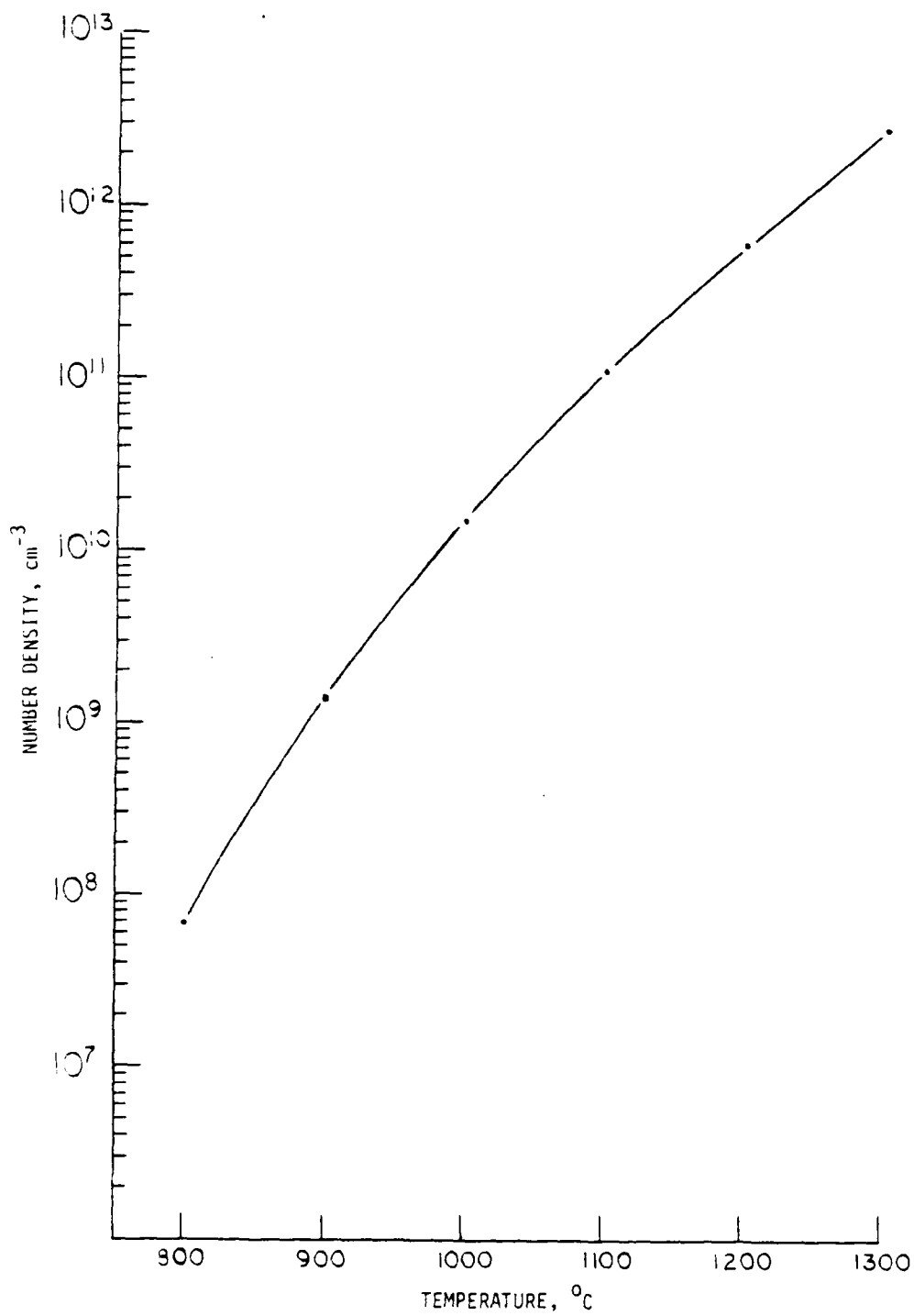


Figure 6. Population of the $6p^2 3P_2$ state of the lead atom as a function of temperature.

which is derived under the assumptions that the population of the upper state of this transition ($6p7s\ ^3P_1$) is negligible relative to the lower and that the line profile is solely determined by Doppler broadening. Then the total absorption was calculated for an assumed 85 cm absorption length in the cell, and the results indicated total absorption at line center should occur with the cell operating at about 900°C.

However, the reliability of such a simple model of the line is not warranted under the conditions of these tests because the pressure of the lead and the buffer gas are very high. At the working pressures here Holtzmark broadening (lead-lead collisions) and Lorentz broadening (lead-other atom collisions) are of significant values. Such collisional broadening effects would produce a line much broader than the Doppler profile with correspondingly greater absorption in the wings of the line.

It was clearly well beyond the scope of this program to pursue line-broadening calculations to evaluate the total line absorption over the temperature range of interest. Therefore, it was decided to implement an appropriate optical system to measure the absorption as a function of temperature. This data would be evaluated to determine the usefulness of this technique for monitoring the lead density in the cell.

The optical system which was assembled is shown schematically in Figure 7. The light source is a tungsten filament lamp (GE 6V, 9A) which has sufficient intensity in the 400 nm range at its normal operating temperature to make an absorption measurement practical. Lenses and apertures having appropriate characteristic dimensions were selected to project a collimated beam 3/4 inch in diameter through the lead vapor cell. After traversing the cell the light is focused on the entrance slit of a half-meter Ebert monochromator. The signal is detected by a 1P28 photomultiplier tube at the exit slit and is recorded on a chart recorder.

A curve-of-growth was generated by loading a cell tube with several beads of lead along the entire length of the hot zone,

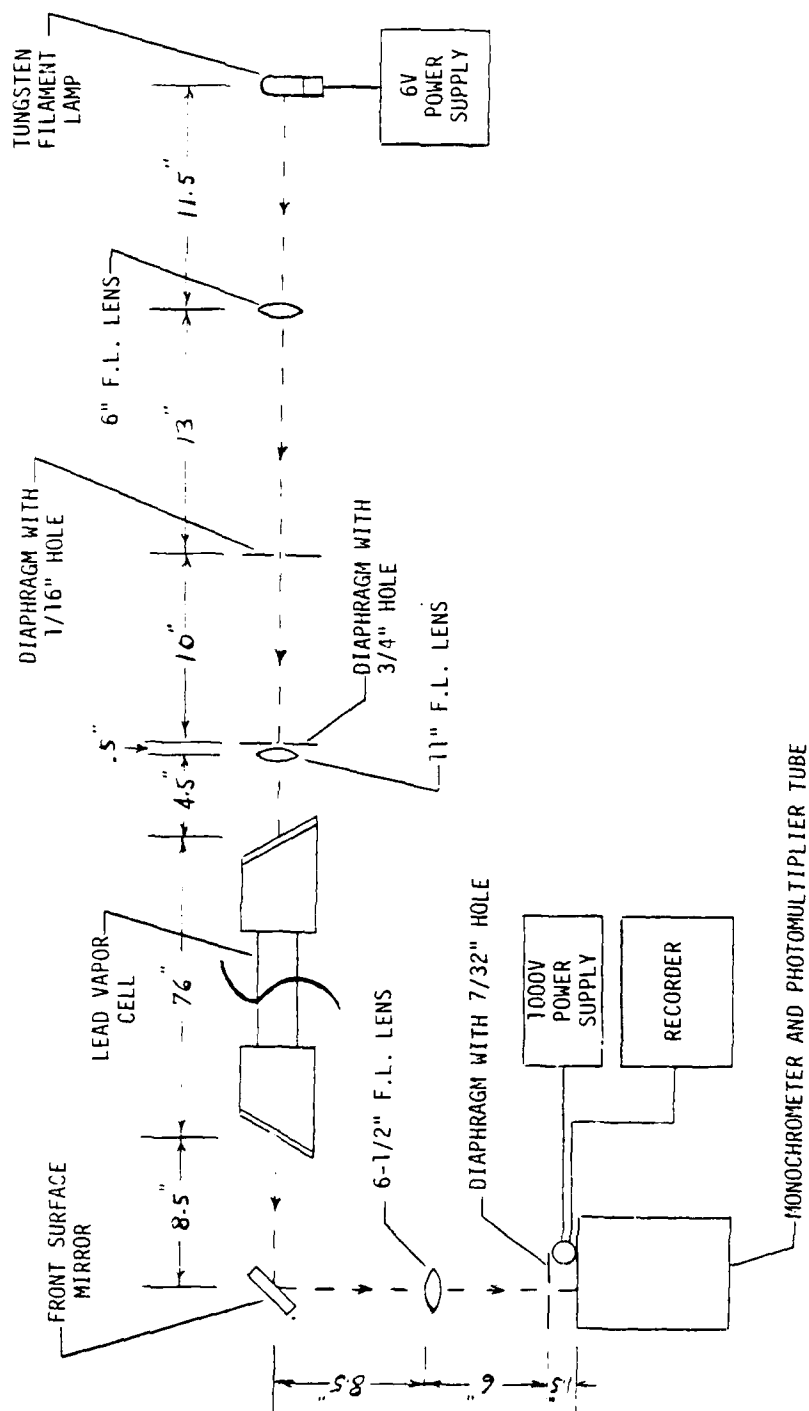


Figure 7. Schematic diagram of the optical system used for the measurement of lead density by optical absorption.

thereby guaranteeing that the cell was filled with lead vapor at the pressure corresponding to a given temperature. The temperature of the furnace was then raised in 100°C increments from its lowest setting of 500°C to the desired operating point of 1300°C. The rate of rise of temperature was limited by the thermal time constant of the furnace and by consideration to minimize thermal shock to all system components. At each temperature setting the absorption profile was measured by scanning the monochromator on its slowest setting (2Å/min) through the 405.7 nm line.

Data on the absorption measurements are listed in Table 2. Detectable absorption was first observed at 800°C. In the 1200-1300°C range the peak absorption is beginning to saturate as a function of temperature (number density) is seen in Figure 8.

TABLE 2. PERCENT ABSORPTION AT 405.7 nm LINE CENTER

BUFFER GAS	TOTAL PRESSURE	TEMPERATURE, °C					
		800	900	1000	1100	1200	1300
He	40 mm	1.2	6.6	15.1	30.7		
He	40-50 mm	1.3	6.8	15.9	33.3	58.7	
He/1% H ₂	190 mm	1.46	8.2	21.8	48.7	77.1	89.0
A/20% H ₂	180 mm	1.72	9.4	23.5	46.0	78.3	90.9
A/20% H ₂	175 mm	1.1	9.2	22.9	46.8	78.3	90.6

The first two rows demonstrated that we could achieve reproducible curves-of-growth from run-to-run with new fillings of lead and the same operating buffer gas pressures. The data in the third row (He/1% H₂) clearly shows that the elevated buffer gas pressure results in more broadening of the line and greater absorption. In the fourth row we show the data after the switch to the argon-hydrogen mix which was used for the first long life test of the tungsten carbide wicks (see Section 4.5). The heavier buffer gas was selected for the life test to minimize the diffusion loss rate of lead and thus increase the operating life, all other factors being equal.

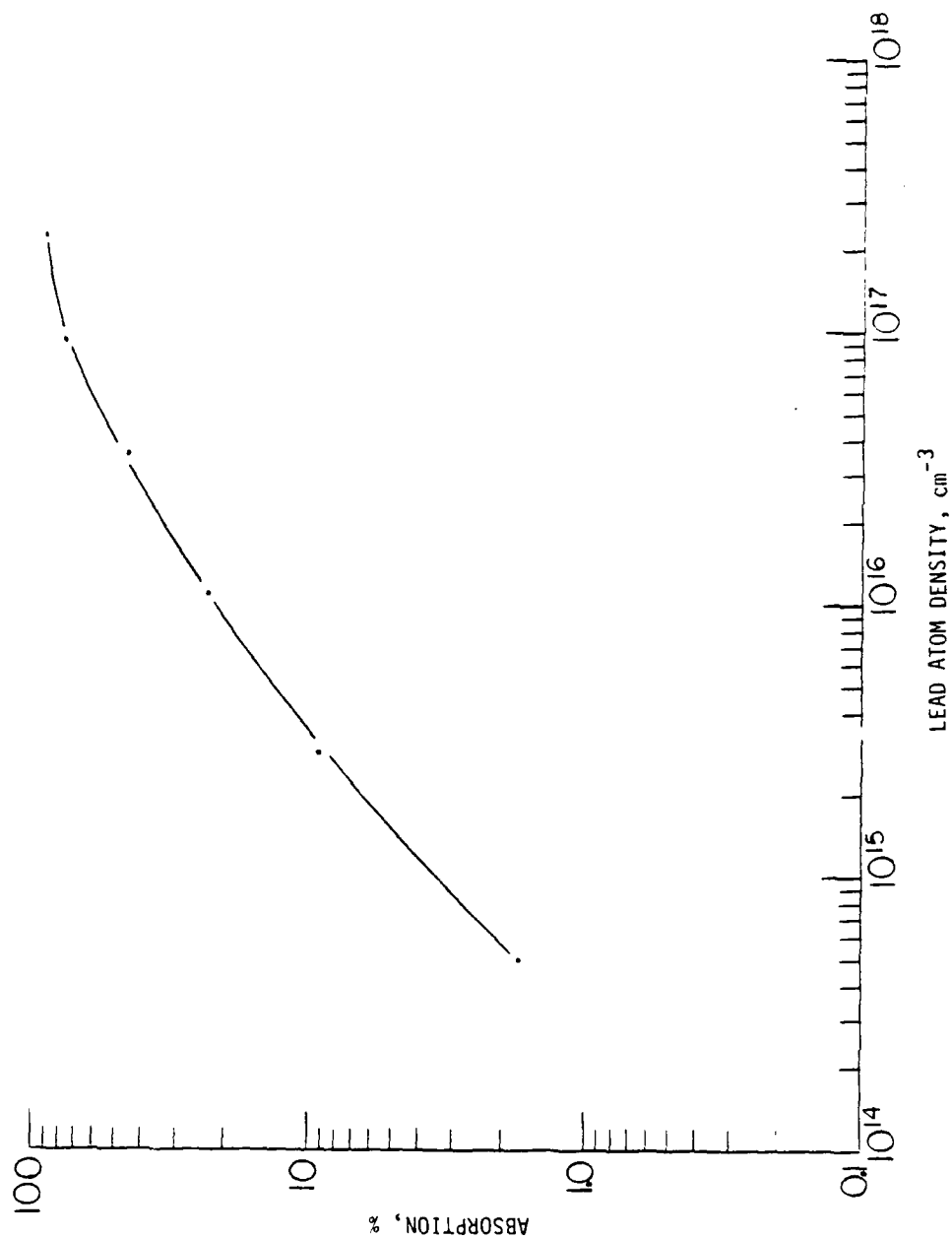


Figure 8. The percent absorption at line center of the 405.7 nm line as a function of lead atom number density.

It is interesting to note that at the lower temperatures the line profile is obviously determined by the monochromator instrument function. Whereas at the high temperatures the line shape was not that of the instrument, particularly in the existence of broad wings. Thus the high degree of broadening must be due to the collisional phenomena mentioned above, because even at 1300°C the Doppler line width is significantly less than the instrumental width. No attempt has been made to investigate this further.

However, we do believe that we have established a satisfactory method for determining and monitoring the lead vapor density as a function of time during operation of the Raman cell.

4.4 CELL PREPARATION

The accumulated experience gained during the development of the metal vapor lasers has demonstrated that proper preparation of the ceramic tube and wick material is required for optimum long term performance.⁽⁴⁾ This is particularly true if a laser is to be run under sealed-off conditions. Since the Raman cell is fabricated with identical materials and is to run sealed-off for long periods, it is obvious that similar materials preprocessing are absolutely necessary.

In general the processing of materials consists of outgassing or baking out at temperatures equal to or exceeding the eventual normal operational values. In most instances for laser applications the bakeout is accomplished under discharge-heating conditions either in a laser assembly itself or in an off-line processing facility. Since a discharge is present the bakeout is not done at a high ultimate vacuum, but rather at 10-20 mm of helium with a slow flow which continuously purges the system.

The recirculating wicks can be processed as part of the tube itself. However, we have also found merit in off-line processing of them. By doing so the wicks can generally be heated more easily to elevated temperatures than they can be when located in their normal position near the ends of a tube. Also there is

greater degree of control over the absolute temperature and the profile when wetting in the metal.

Typically the materials will be baked out for approximately 43 hours. In the case of the wicks about one-half of this time will be with helium as the principal buffer gas and a small percentage (0.5-2.0%) admixture of hydrogen. The presence of hydrogen in the discharge greatly facilitates the wetting in of the metal presumably by its effects in reducing any oxides which have formed on the surface of the wicking material.

In this program the ceramic tubes were baked-out at 1350°C under low pressures (≤ 5 μ m) in the high temperature furnace facility. Their extreme length (72 inches) precluded off-line processing because a special facility would have had to be constructed. Bakeout times were in the 60-90 hour range.

The wicks were processed in an off-line facility. Though they are 2 inches longer than a typical metal vapor laser wick, they were easily accommodated in an existing facility. The wicks were located in the center and on-axis of a large diameter discharge tube and heated to 1300°C for 40-60 hours. Approximately 1/3 to 1/2 of this time was with a helium/hydrogen mix. They were then cooled, pulled out towards the ends of the tube, loaded with beads of lead and heated up to the 600-700°C range. Discharge heating with a helium/hydrogen mix was used. Lead was loaded in 5 to 10 steps over several days time until they were well wet and saturated. The wicks were then removed from the processing facility and loaded into the Raman cell tube for testing.

4.5 LEAD VAPOR CELL TEST PROGRAM

During the test phase of this program four cells were processed, assembled and tested using two different wicking materials. The fourth and final cell tested operated at a pd of 1.4×10^{19} /cm² for 835 hours before the test was terminated in order to prepare a new cell and all the hardware for delivery. The corresponding contract goals were $pd = 1.2 \times 10^{19}$ /cm² and an operating time of 500 hours.

A fifth cell was prepared for delivery, and its performance during burn-in operation certainly suggests that the long life operation will be reproducible. These tests will be described in greater detail in the remainder of this section.

The first two cells which were assembled had their testing prematurely terminated because of the occurrence of numerous cracks which developed in the wall of the ceramic cell tube. In the first case one or more of these cracks actually penetrated the wall of the tube causing a vacuum leak. Thus no further testing could be done, and this cell was removed from the furnace.

In the second case the tube fractured when some slight mechanical stress was placed on it. Both of these failures occurred early in the test before any data on wick performance could be obtained. Though the exact cause of the failure was never positively identified, the problem never recurred after a second ceramic tube was placed over the main cell tube to protect it from looking directly at the interior of the furnace.

The third cell produced the first significant test of wick performance. Wicks consisting of tungsten plasma sprayed on a tantalum substrate and a cell tube were processed separately as described in Section 4.4. After the tube was cooled to room temperature the wicks were positioned in the tube, and the central region between the wicks was loaded with several small pieces of lead.

The cell and lines were evacuated, and the furnace was heated to 500°C with the tube under vacuum. The cell was then valved off, filled to a total pressure of 190 mm of He/1% H_2 and heated to 800°C . The cell was allowed to idle over night at these conditions.

The temperature of the furnace was then raised to the operating value (1300°C) in 100°C increments at approximately half-hour intervals. The optical absorption on the 405.7 nm line of atomic lead was measured at equilibrium at each value of temperature beginning with the point of detectable absorption at 800°C . This absorption data is recorded in line 3 of Table 2.

A maximum absorption of 89.0% was measured immediately after reaching equilibrium at 1300°C. Approximately 1-1/2 hours later the absorption had fallen to 84.8%. During this decay a definite small step decrease was observed as the last small bead of lead disappeared from the center of the tube. The decay in absorption, and hence lead density, continued monotonically over the next several hours. Therefore, the test was terminated.

The system was cooled to room temperature, and the wicks and tube were reloaded with lead. The furnace was heated to 1300°C on a similar schedule with a He/15%H₂, and the absorption was monitored as above. A similar pattern of results was obtained implying that the wicks were not wetting well enough to confine the lead vapor and maintain the proper vapor density. Therefore this cell was removed from the furnace facility, and another cell was processed.

The wicks made with a tungsten carbide wetting surface on a tantalum substrate were selected for the fourth test cell. The ceramic tube and wicks were processed separately before the wicks were inserted into the cell. The center zone of the tube was loaded with several small pieces of lead before it was evacuated. The cell was then filled with a mixture of A/20%H₂ to a pressure of 180 mm. The switch to argon from helium was made in order to have a heavier buffer gas to reduce the diffusion of lead and thereby increase operating life. The cell was heated to 1300°C on a schedule essentially identical to that described above.

The absorption on the 405.7 nm line was measured at 100°C intervals from 800°C to 1300°C. This data is recorded as line 4 in Table 2. A maximum absorption of 90.9% was recorded immediately after reaching equilibrium at 1300°C. From Figure 5 it can be seen that this corresponds to a number density of $2.2 \times 10^{17}/\text{cm}^3$. During the next 18 hours the absorption fell to approximately 89.0% (Figure 9). This corresponds to a decrease in lead density to about $1.75 \times 10^{17}/\text{cm}^3$.

However, the cell then continued to operate at essentially this lead density for a period of 835 hours. The line absorption

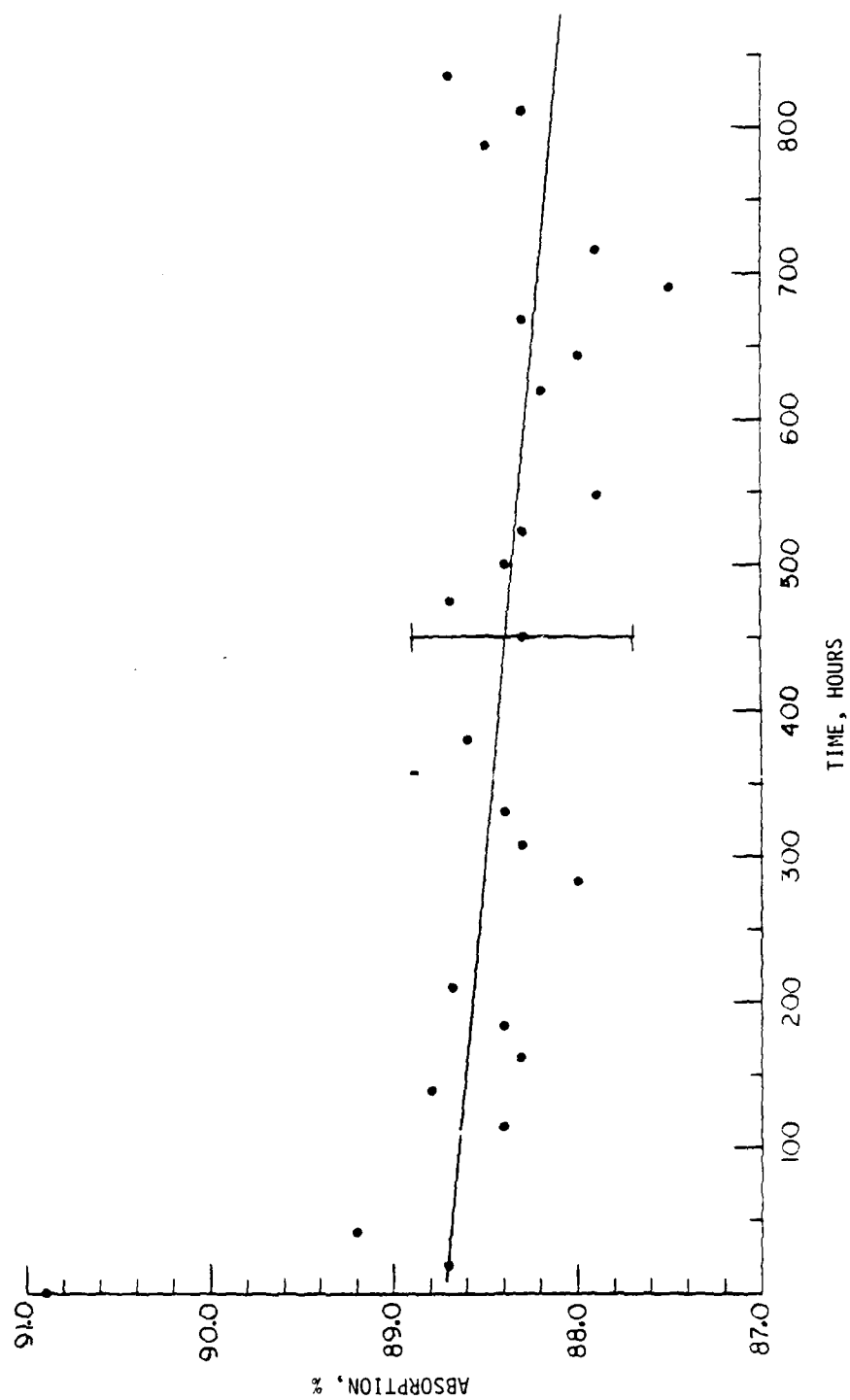


Figure 9. The percent absorption as a function of time during the 835-hour life test.

as a function of time for the run is plotted in Figure 9. A straight line has been fit to the data (with the exception of the point at $t=0$) using the least squares method. This straight line predicts a value of 88.7% absorption at $t=0$ and 88.1% at $t=835$ hours. This corresponds to a decrease from $1.7 \times 10^{17}/\text{cm}^3$ to $1.6 \times 10^{17}/\text{cm}^3$ over the course of the run. If we project this line to 10,000 hours operating time the absorption would be 81.8% corresponding to a density of $1.1 \times 10^{17}/\text{cm}^3$.

The estimated hot zone length during the test was 85 cm which gives a pd value varying from $1.45 \times 10^{19}/\text{cm}^2$ to $1.36 \times 10^{19}/\text{cm}^2$ over the course of the run. If we select the contract goal of $\text{pd}=1.2 \times 10^{19}/\text{cm}^2$ as the definition of minimum condition for useful operating life, then the curve of Figure 9 gives a value of 3900 hours. If the useful life criteria is lowered to $1.0 \times 10^{19}/\text{cm}^2$, a factor of 20% below the contract goal, then the predicted operating life is 7500 hours. In either case the performance of the cell during this test clearly exceeds the contract goals by a significant margin.

Following the necessary, but unfortunately premature, termination of the very successful test another identical tube was prepared for delivery. After materials processing and assembly the tube was taken up to the specified operating condition. The optical absorption data for this burn-in are shown in line 5 of Table 2. It is clear that the performance is identical within experimental uncertainties to the previous long life cell. Also after having been in a stable condition at 1300°C for about 17 hours, the cell was taken through a thermal cycle down to 1000°C and returned to 1300°C . Performance was not degraded by the cycle. The tube was run for a total of 113 hours before the system was disassembled for shipment. Thus we have good indications that both reproducibility and thermal cycling can be obtained.

5.0 CONCLUSIONS AND RECOMMENDATIONS

The operational life test of the lead vapor Raman cell which was conducted on the current contract exceeded the contract goal of 500 hours by a significant margin (67%) despite the fact that the test was prematurely terminated before the actual usable life was experimentally determined. However, projections based on an extrapolation of the data gathered during the test indicate that multi-thousand hour operation is easily within reach. Thus a high temperature lead vapor Raman cell is clearly a viable device for frequency down-conversion of XeCl laser radiation for either ground-based or space-based systems applications.

The next phase of this development program should address the issues of reproducibility and the determination of the actual usable life of the current wick designs. Materials processing procedures need refinement, and criteria for identifying that materials have successfully passed the processing stage must be developed to a higher degree.

A parallel effort should begin the design and evaluation of the next generation of wicks for very long life operations (five years). Two design concepts exist at present and would warrant immediate attention in follow-on work.

This continued testing must be supported by the development of a computer code to model the wick performance for this type of application. Verification of the model would be accomplished by parametric studies using current cell designs. Such a model is absolutely required to predict cell performance out to five years for various design concepts since tests of that duration are obviously not practical.

Finally, the level of performance is already such that engineering design studies should be undertaken to define the systems concepts for ground-based, airborne or space-based applications.

ACKNOWLEDGMENTS

It is a pleasure to acknowledge the assistance of several people who made significant contributions to the success of this program. Mr. A. E. Kreft set up and carried out all the materials processing and laboratory tests during the program. He is also responsible for all the drafting work for the figures contained herein.

Mr. L. W. Springer was responsible for the installation of the furnace, and he also headed the effort which solved the heater rod breakage problem.

The assistance of Ms. G. R. Vecchiolli in the typing and handling of other details necessary to prepare this report is appreciated.

Finally, the ready availability of Mr. R. J. Homsey, Manager of Laser Programs, for discussions and advice throughout this program was instrumental in its success.

REFERENCES

1. R.Burnham and E.Schimitschek, "High Power Blue-Green Lasers," Laser Focus 17, 54 (1981).
2. R.Burnham and N.Djeu, "Efficient Raman Conversion of XeCl-Laser Radiation in Metal Vapors," Optics Letters 3, 215 (1978).
3. B.G.Bricks, "Development of the Discharge-Heated Lead Vapor Laser," AFAL-TR-78-103, Air Force Avionics Laboratory, Wright-Patterson AFB, OH 45433, 1978.
4. T.W.Karras and B.G.Bricks, "Metal Vapor Laser Contaminant Study," GE TIS No. 80SDS028, October 1980.
5. R.E.Honig and D.A.Kramer, "Vapor Pressure Data for the Solid and Liquid Elements," RCA Review, 296 (June 1969).

APPENDIX
INSTALLATION/OPERATION INSTRUCTIONS

1. Assemble/install furnace as per Lindberg instruction manual.
2. Perform initial furnace bake-out as per said manual.
3. Cool furnace to room temperature.
4. Assemble/install lead vapor Raman cell in furnace using Figure 1 of this report as a guide.
 - 4.1 Insert large diameter ceramic tube into furnace with two inner ceramic support rings. Position rings over support stands and then insert outer ceramic support rings into firebrick end walls of furnace.
 - 4.2 Insert main cell tube and support with ceramic rings in firebrick end walls and put insulation sleeves into place.
 - 4.3 Install window assemblies.
 - 4.4 Assemble vacuum lines/hardware and connect to window assemblies.
5. Pump out and leak check (if possible) with helium leak checker.
6. After cell has pumped down to 10-15 microns, set furnace at 500°C. Allow system to idle overnight at 500-700°C while pumping on cell.
7. Valve off cell and fill to 180-200 mm of A/20%H₂ mixture.
8. Increase temperature to desired operating point in 50 or 100°C increments. Rates of ~150°C/hr have been done with no apparent thermal shock problems.